Turkish Journal of Electrical Engineering & Computer Sciences

http://journals.tubitak.gov.tr/elektrik/

Research Article

Turk J Elec Eng & Comp Sci
(2016) 24: 4142 – 4153

doi:10.3906/elk-1501-110

Development of derivation of inverse Jacobian matrices for 195 6-DOF GSP mechanisms

Metin TOZ[1,*], **Serdar KÜÇÜK**[2]
[1]Department of Computer Engineering, Faculty of Technology, Düzce University, Düzce, Turkey
[2]Department of Biomedical Engineering, Faculty of Technology, Kocaeli University, Kocaeli, Turkey

Received: 16.01.2015 • **Accepted/Published Online:** 18.07.2015 • **Final Version:** 20.06.2016

Abstract: One of the key issues in robotics is finding high-performance manipulator structures. To evaluate the performance of a parallel manipulator, researchers mostly use kinematic performance indices (such as condition number, minimum singular value, dexterity, and manipulability), which are based on inverse Jacobian matrices. Driving the inverse Jacobian matrix of even one parallel manipulator is a very cumbersome process. However, in this paper, general equations for the inverse Jacobian matrices of 195 GSP mechanisms are symbolically derived by considering 4 basic leg types having 1 angular and 4 distance constraints. With the help of these general equations, the development of the inverse Jacobian matrix for a GSP mechanism can be achieved by defining only the leg connection points on the base and moving platforms with minimum cost. Having derived the inverse Jacobian matrices, one can directly compute kinematic performance indices to measure and compare the manipulator performance of the 195 GSP mechanism. These analyses may yield new high-performance GSP mechanisms for use in engineering, medical device design, and other applied branches. Two different mechanisms (symmetrical and asymmetrical) are given as examples to describe the methodology for deriving the inverse Jacobian matrices. Finally, 2 numerical examples are given for illustrating the practical applications of the procedure.

Key words: Inverse Jacobian matrix, parallel manipulators, angular and distance constraints, 6-DOF

1. Introduction

Over the last decade, designing new types of parallel robot mechanisms has very much attracted the interest of the robotics research community. Although there have been several studies conducted on the classification and enumeration of topological structures of parallel robot mechanisms in the literature, the type synthesis problem of parallel robot mechanisms has not been fully solved yet [1]. Type synthesis aims to find all possible types of novel parallel robot mechanisms. Gao et al. [2] used distance (D) and/or angular (A) constraints between pairs of points, lines, and/or planes located on the base and moving platforms in order to classify these manipulators. They classified 6 degrees of freedom (6-DOF) GSP mechanisms into 4 groups, namely, 6D, 5D1A, 4D2A, and 3D3A, where D and A mean distance and angular constraints, respectively. The names of the classes identify the types and numbers of the constraints used, e.g., 3D3A is the class of 6-DOF GSP mechanisms that are constructed by using 3 distance and 3 angular constraints between their base and moving platforms. Gao et al. [2] showed that there are 3850 types of 6-DOF GSP mechanisms. Furthermore, several researchers have been interested in these manipulators. Gan et al. [3,4] designed a new 3CCC (cylindrical–cylindrical–cylindrical)

*Correspondence: metintoz@duzce.edu.tr

6-DOF parallel mechanism that has 3 legs between its base and moving platforms. Each leg has 2 active joints, which are located between 2 passive cylindrical joints. One of the active joints has a distance actuator, while the other has an angular actuator. They solved the forward kinematics and the Jacobian matrix of the new 3CCC mechanism. Toz and Kucuk [5] performed the dimensional optimization of the mechanism proposed by Gan et al. [3,4] and showed that the mechanism has better dexterous workspace characteristics than the traditional GSP manipulator. Luo et al. [6,7] proposed a new method for solving the forward kinematics of 4SPS–2CCS and 5SPS–1CCS mechanisms using quaternions, where S and P denote spherical and prismatic joints, respectively. They first searched the initial point provided by a hyperchaotic circuit system and then computed all real solutions of nonlinear equations using the Newton iterative method. In another study, Luo et al. [8] used the hyperchaotic Newton-downhill method to solve the forward kinematic problem of a 3SPS–3CCS type GSP mechanism. All of the above studies were focused on only one single type of 3850 GSP mechanism. On the other hand, Toz and Kucuk [9] proposed a criterion to achieve feasible structures among the 3850 GSP mechanisms. This criterion disregards planar joints, which are not used in practical applications [9]. Thus, 3850 GSP mechanisms are reduced to 195 GSPs, which include 191 asymmetrical and 4 symmetrical GSP mechanisms.

In this study, general inverse kinematics equations of the 195 6-DOF GSP mechanisms were first obtained symbolically by using 4 basic types of legs considering 1 angular and 4 distance constraints, which were defined between geometric primitives arbitrarily located on the base and moving platforms. Subsequently, the inverse Jacobian matrices of the 195 6-DOF GSP mechanisms were symbolically derived. It is well known that the inverse Jacobian matrix provides an instantaneous transformation between joint velocities and linear and angular velocities of the end-effector [5]. It can be used in several analysis processes of these mechanisms, such as the performance evaluation [9–14] and dynamical analysis [15]. A condition number based on the maximum and minimum singular values of the inverse Jacobian matrix is computed in general for performance evaluation of parallel manipulators [16–19]. However, an inconsistency problem between elements of the inverse Jacobian matrix arises when computing the condition number. To overcome this problem, a dimensionally homogeneous inverse Jacobian matrix was also obtained for 195 6-DOF GSP mechanisms. Finally, 2 numerical examples are provided for demonstrating the practical usefulness of the symbolically derived inverse Jacobian matrices.

2. GSP mechanisms

Distance and/or angular constraints between the base and moving platforms can be used for designing 6-DOF GSP mechanisms [2]. The constraints can be defined between the pairs of geometric primitives (point, line, and plane) that are arbitrarily located on the base and moving platforms [2]. Gao et al. [2] used these distance and angular constraints for categorizing GSP mechanisms into 4 classes, namely 6D, 5D1A, 4D2A, and 3D3A. Toz and Kucuk [9] ignored the constraints defined by means of the plane geometric primitives due to their inconvenience [9]. They used the remaining constraints (1 angular and 4 distance constraints) to design 6-DOF of GSP mechanisms. These constraints were named D_1, D_2, D_3, D_4, and A_1 for the point–point distance constraint, line–point distance constraint, point–line distance constraint, line–line distance constraint, and line–line angular constraint, respectively. According to these constraint types, Toz and Kucuk [9] reduced the possible combinations of GSP mechanisms from 3850 to 195 using the same combination formula used by Gao et al. [2]. They also grouped 195 GSP mechanisms into 6D, 5D1A, 4D2A, and 3D3A classes [9]. Four types of legs illustrated in Figure 1 can be used for forming these constraints. The D_1 type constraint, defined between 2 points located on the base and moving platforms, can be obtained by using the S$\underline{\text{P}}$S type leg illustrated in

Figure 1a. The S$\underline{\text{P}}$S type leg has 2 spherical passive joints attached to each end of the active prismatic joint. The D_2 type constraint was obtained by using the S$\underline{\text{P}}$C type leg illustrated in Figure 1b, while the D_3 type constraint was obtained by a C$\underline{\text{P}}$S type leg demonstrated in Figure 1c, where C shows the cylindrical joint. D_4 and A_1 type constraints were defined between 2 lines. Therefore, the C$\underline{\text{C}}$C type leg shown in Figure 1d can form both D_4 and A_1 type constraints. A cylindrical joint comprises a prismatic and a revolute joint that slides along and rotates around the same axis, respectively. It should be noted that the active joint of the C$\underline{\text{C}}$C type leg for the D_4 type constraint was determined as the prismatic part of the second cylindrical joint, while the active joint of the C$\underline{\text{C}}$C type leg for the A_1 type constraint was the revolute part of the second cylindrical joint. Active joints are indicated by underlying the corresponding joint symbol. For example, prismatic joint P is underlined in order to show the active joint in the S$\underline{\text{P}}$S type leg. All 195 symmetrical and asymmetrical GSP mechanisms can be constructed by using the 4 types of legs given in Figure 1. A symmetrical GSP mechanism constructed using 6 D_1 type constraints is given in Figure 2a, and an asymmetrical mechanism that has 5 D_3 and 1 D_4 constraints between its platforms is given in Figure 2b.

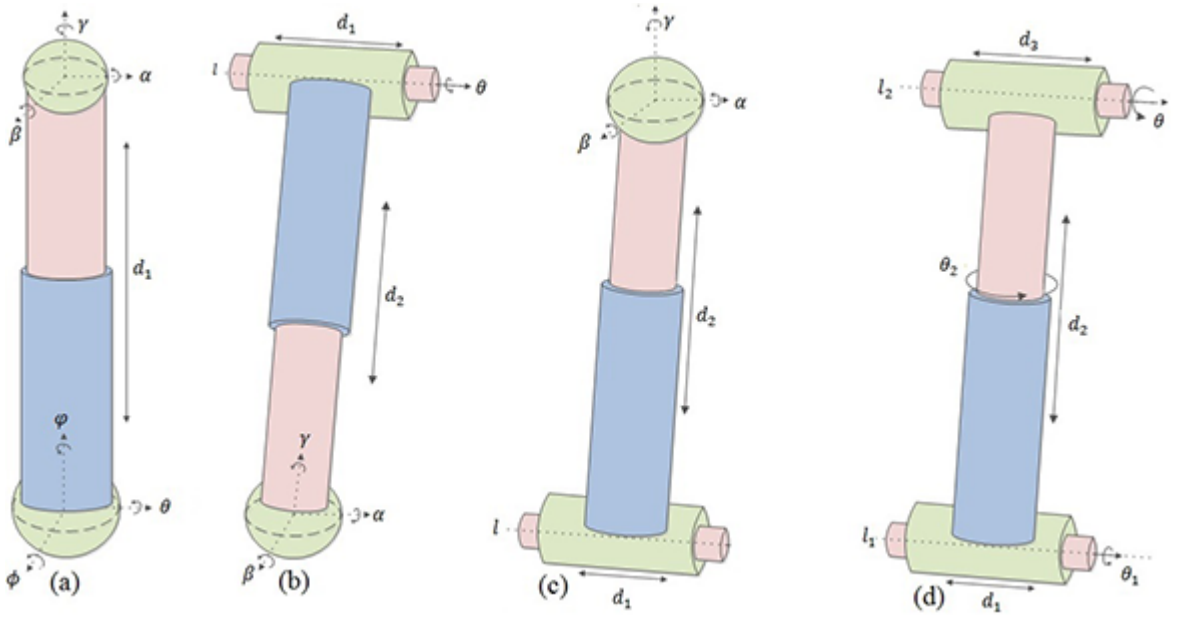

Figure 1. a) S$\underline{\text{P}}$S type leg for D_1; b) S$\underline{\text{P}}$C type leg for D_2; c) C$\underline{\text{P}}$S type leg for D_3; d) C$\underline{\text{C}}$C leg type for D_4 and A_1 type constraints.

3. Inverse kinematics

In this section, the inverse kinematics of GSP mechanisms are presented. Since 195 GSP mechanisms can be built by using the 4 types of legs given in Figure 1, kinematic equations were derived by considering these 4 leg types. $O(x, y, z)$ and $P(u, y, w)$ are coordinate systems located on the base and moving platforms, respectively. All 4 leg types can be mounted on the base and moving platform as illustrated in Figure 3. In the figure, A_i, A_j and B_i, B_j are arbitrarily selected points on the base and moving platforms, respectively, and K_i and L_i are the lines that passing through these 2 pairs of points. The position vectors of the A_i, A_j and B_i, B_j points are $\vec{a}_i$, $\vec{a}_j$ and $\vec{b}_i$, $\vec{b}_j$ according to the O and P coordinate systems, respectively, while $\vec{P}$ is the position vector between the centers of the 2 coordinate systems. Finally, d_i and θ_i are the distance and angle constraints provided by the active prismatic and angular actuators, respectively.

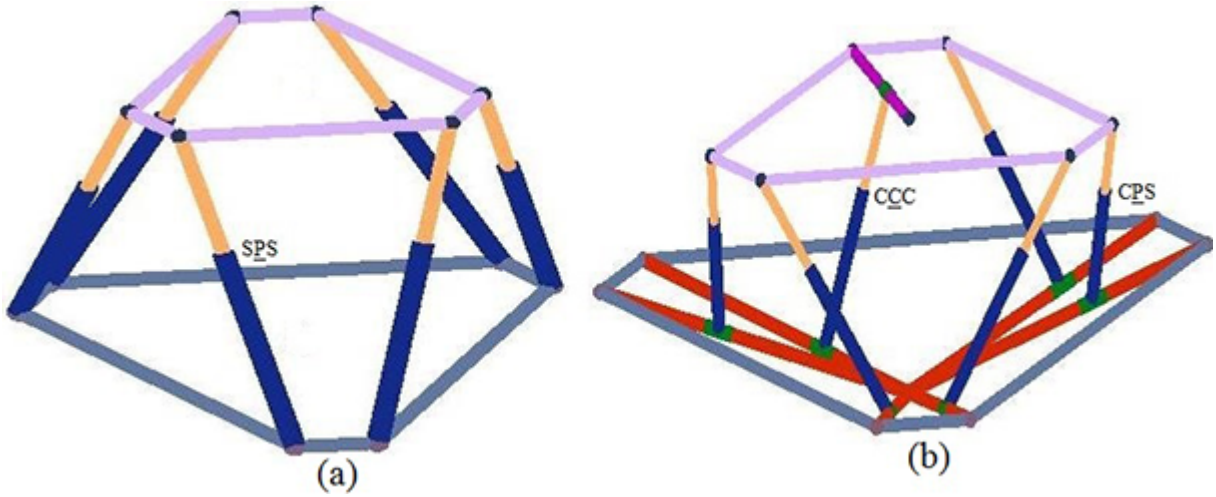

Figure 2. a) Symmetrical GSP mechanism constructed using 6 D_1 type constraints; b) asymmetrical GSP mechanism constructed using 5 D_3 and 1 D_4 constraints.

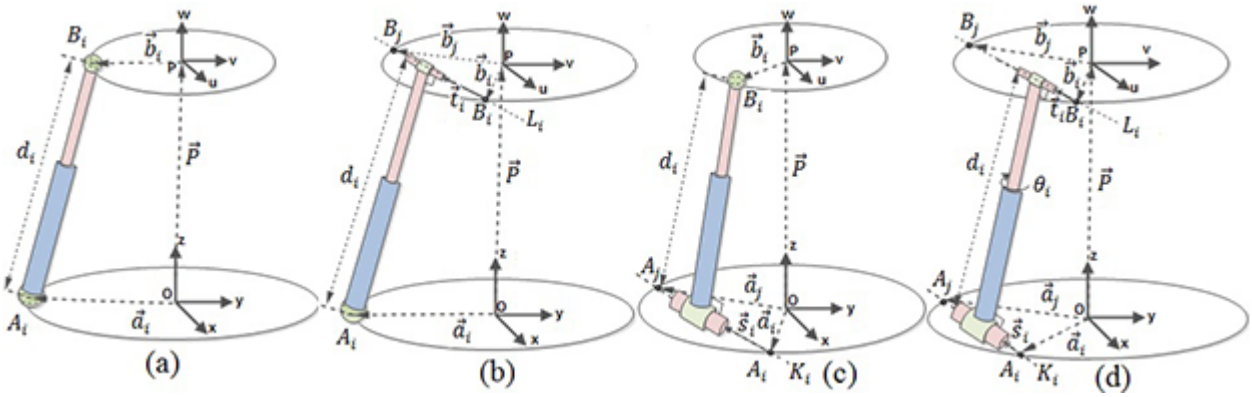

Figure 3. a) SPS type leg for D_1 type constraint; b) SPC type leg for D_2 type constraint; c) CPS type leg for D_3 type constraint; d) CCC type leg for D_4 and A_1 type constraints.

3.1. Inverse kinematics for the D_1 type constraint

As described in the previous section, the D_1 type constraint can be obtained by using the SPS type leg illustrated in Figure 1a. The SPS type leg is one of the most preferred leg types used in Stewart–Gough platform-type mechanisms. An SPS type leg can be mounted on the base and moving platform as illustrated in Figure 3a. According to the figure, the $\vec{d_i}$ vector can be written as follows:

$$\vec{d_i} = \vec{P} + R\vec{b_i} - \vec{a_i}, \tag{1}$$

where R is the rotation matrix of the end-effector in terms of the O coordinate system and defined by using the $R_{XYZ}(\alpha, \beta, \gamma)$ roll, pitch, and yaw angle set. The norm of the $\vec{d_i}$ vector given in Eq. (1) can be used as the inverse kinematic equation of the SPS type leg where $\cdot$ is the dot product of 2 vectors [2].

$$d_i^2 = \left(\vec{P} + R\vec{b_i} - \vec{a_i}\right) \cdot \left(\vec{P} + R\vec{b_i} - \vec{a_i}\right). \tag{2}$$

3.2. Inverse kinematics for the D_2 type constraint

The D_2 type constraint can be obtained by using an S$\underline{P}$C type leg, as demonstrated in Figure 3b. It should be noted that the active prismatic joint is perpendicular to the cylindrical joint and L_i. By using the identities in the figure, the inverse kinematics for the S$\underline{P}$C type leg can be obtained as follows [2]:

$$d_i^2 = \left(\left(\vec{P} + R\vec{b_i} - \vec{a_i}\right) \times R\vec{t_i}\right) \cdot \left(\left(\vec{P} + R\vec{b_i} - \vec{a_i}\right) \times R\vec{t_i}\right), \tag{3}$$

where $\vec{t_i} = \frac{\vec{b_j} - \vec{b_i}}{\left|\vec{b_j} - \vec{b_i}\right|}$ and $|\,|$ is the norm of a vector.

3.3. Inverse kinematics for the D_3 type constraint

The D_3 type constraint can be obtained by a C$\underline{P}$S type leg as drawn in Figure 3c, and the inverse kinematic equation can be obtained as follows, where $\vec{s_i} = \frac{\vec{a_j} - \vec{a_i}}{|\vec{a_j} - \vec{a_i}|}$ [2]:

$$d_i^2 = \left(\left(\vec{P} + R\vec{b_i} - \vec{a_i}\right) \times \vec{s_i}\right) \cdot \left(\left(\vec{P} + R\vec{b_i} - \vec{a_i}\right) \times \vec{s_i}\right). \tag{4}$$

3.4. Inverse kinematics for the D_4 type constraint

The D_4 type constraint can be obtained by a C$\underline{C}$C type leg as drawn in Figure 3d. By using the identities in Figure 3d, the inverse kinematic equation of the C$\underline{C}$C type leg for the D_4 type constraint can be defined by using the following equation [2]:

$$d_i^2 = \frac{\left(\left(\vec{P} + R\vec{b_i} - \vec{a_i}\right) \cdot \left(R\vec{t_i} \times \vec{s_i}\right)\right)^2}{\left(R\vec{t_i} \times \vec{s_i}\right) \cdot \left(R\vec{t_i} \times \vec{s_i}\right)}. \tag{5}$$

3.5. Inverse kinematics for the A_1 type constraint

The A_1 type constraint illustrated in Figure 4 can be described as the angle between lines passing through the axes of the first and last cylindrical joints of the C$\underline{C}$C type leg [2].

$$\cos\theta_i = R\vec{t_i} \cdot \vec{s_i} \tag{6}$$

In Figure 4, θ_i is the angle between 2 unit vectors parallel to K_i and L_i. It should be noted that all of the inverse kinematic equations derived in this section were also obtained by means of Lazard's and Mourrain's coordinate systems in [2].

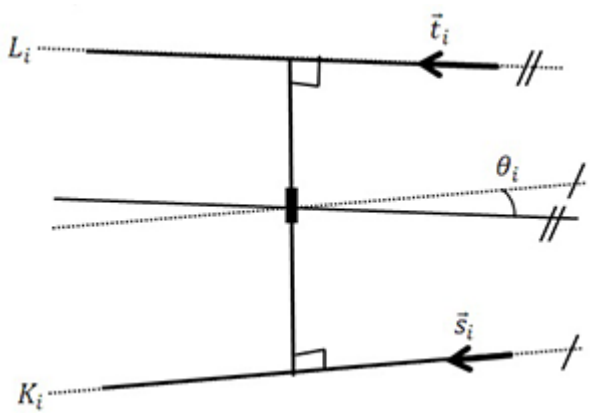

Figure 4. An illustration of C$\underline{\text{C}}$C type leg building the A_1 type constraint.

4. Inverse Jacobian matrix

The Jacobian matrix of a 6-DOF parallel robot manipulator given by Eq. (7) provides a relationship between active joint variables and linear and angular velocities of the manipulator end-effector [20]:

$$\begin{bmatrix} v_p & \omega_p \end{bmatrix}^T = J \begin{bmatrix} \dot{\rho}_1 & \cdots & \dot{\rho}_6 \end{bmatrix}^T, \tag{7}$$

where $v_p = \begin{bmatrix} v_{p_x} & v_{p_y} & v_{p_z} \end{bmatrix}^T$ and $\omega_p = \begin{bmatrix} \dot{\alpha} & \dot{\beta} & \dot{\gamma} \end{bmatrix}^T$ are linear and angular velocities of the end-effector, respectively, and $\dot{\rho}_i (i = 1 \cdots 6)$ are the time derivatives of the active joint variables. J is the Jacobian matrix of the mechanism. Since analytical derivation of the forward Jacobian matrix is almost impossible [20], the inverse Jacobian matrix is commonly derived for 6-DOF parallel manipulators:

$$\begin{bmatrix} \dot{\rho}_1 & \cdots & \dot{\rho}_6 \end{bmatrix}^T = J^{-1} \begin{bmatrix} v_p & \omega_p \end{bmatrix}^T, \tag{8}$$

where J^{-1} is the inverse Jacobian matrix of a 6-DOF parallel manipulator. The inverse Jacobian matrix of the GSP mechanisms is one of the most important factors for the design and performance evaluations of parallel robot mechanisms and can be obtained by writing the time derivatives of the inverse kinematic equations. Therefore, inverse Jacobian matrices for the 195 GSP mechanisms can be developed by performing time derivatives of the inverse kinematic equations for each constraint type. Moreover, general row vectors can be defined for all the constraint types to obtain the inverse Jacobian matrices of the GSP mechanisms as follows.

4.1. General row vectors for all the constraint types

The time derivative of Eq. (2) can be written as follows:

$$\dot{d}_i = \frac{1}{d_i} \left(\omega_p \times R\vec{b}_i + v_p \right) \cdot \left(\vec{P} + R\vec{b}_i - \vec{a}_i \right). \tag{9}$$

The linear and angular velocities in Eq. (9) should be decoupled in order to obtain the row vector of the inverse Jacobian matrix for the D_1 type constraint:

$$\dot{d}_i = \frac{1}{d_i} \left(\left(\vec{P} + R\vec{b}_i - \vec{a}_i \right) \cdot v_p + \left(R\vec{b}_i \times \left(\vec{P} + R\vec{b}_i - \vec{a}_i \right) \right) \cdot \omega_p \right). \tag{10}$$

Eq. (10) can be reorganized as follows:

$$\dot{d}_i = J_{D_1} \begin{bmatrix} v_p & \omega_p \end{bmatrix}^T, \tag{11}$$

where J_{D_1} is the row vector that can be used for obtaining the inverse Jacobian matrix of a GSP mechanism that includes an S$\underline{\text{P}}$S type leg and is defined as follows:

$$J_{D_1} = \frac{1}{d_i} \left[\left(\vec{P} + R\vec{b}_i - \vec{a}_i \right)^T \left(R\vec{b}_i \times \left(\left(\vec{P} + R\vec{b}_i - \vec{a}_i \right) \right) \right)^T \right]. \tag{12}$$

General row vectors for the other constraint types can be written by using the same procedure with the D_1 type constraint as follows:

$$J_{D_2} = \frac{1}{d_i} \begin{bmatrix} \varepsilon_{v_p} & \varepsilon_{\omega_p} \end{bmatrix}, \tag{13}$$

where:

$$\varepsilon_{v_p} = \left(R\vec{t}_i \times \left(\left(\vec{P} + R\vec{b}_i - \vec{a}_i \right) \times R\vec{t}_i \right) \right)^T$$

$$\varepsilon_{\omega_p} = \left(\left(\left(\vec{P} - \vec{a}_i \right) \cdot R\vec{t}_i \right) \left(\left(\vec{P} + R\vec{b}_i - \vec{a}_i \right) \times R\vec{t}_i \right) \right)^T + \left(\left(\left(\left(\vec{P} + R\vec{b}_i - \vec{a}_i \right) \times R\vec{t}_i \right) \cdot R\vec{b}_i \right) R\vec{t}_i \right)^T$$

$$J_{D_3} = \frac{1}{d_i} \left[\left(\vec{s}_i \times \left(\left(\vec{P} + R\vec{b}_i - \vec{a}_i \right) \times \vec{s}_i \right) \right)^T \left(\left(\left(\left(\vec{P} + R\vec{b}_i - \vec{a}_i \right) \times \vec{s}_i \right) \times \vec{s}_i \right) \times R\vec{b}_i \right)^T \right], \tag{14}$$

$$J_{D_4} = \frac{1}{n_i} \begin{bmatrix} \varepsilon_{v_p} & \varepsilon_{\omega_p} \end{bmatrix}, \tag{15}$$

where:

$$n_i = d_i \left(\left(R\vec{t}_i \times \vec{s}_i \right) \cdot \left(R\vec{t}_i \times \vec{s}_i \right) \right)$$

$$\varepsilon_{v_p} = \left(\left(\left(\vec{P} + R\vec{b}_i - \vec{a}_i \right) \cdot \left(R\vec{t}_i \times \vec{s}_i \right) \right) \left(R\vec{t}_i \times \vec{s}_i \right) \right)^T$$

$$\varepsilon_{\omega_p} = \left(\left(\left(\vec{P} + R\vec{b}_i - \vec{a}_i \right) \cdot \left(R\vec{t}_i \times \vec{s}_i \right) \right) \left(\left(R\vec{b}_i \cdot \vec{s}_i \right) R\vec{t}_i - \left(R\vec{b}_i \cdot R\vec{t}_i \right) \vec{s}_i \right) \right)^T$$

$$+ \left(\left(\left(\vec{P} + R\vec{b}_i - \vec{a}_i \right) \cdot \left(R\vec{t}_i \times \vec{s}_i \right) \right) \left(\left(-\vec{s}_i \cdot R\vec{t}_i \right) \left(\vec{P} + R\vec{b}_i - \vec{a}_i \right) \right) \right)^T$$

$$+ \left(\left(\left(\vec{P} + R\vec{b}_i - \vec{a}_i \right) \cdot \left(R\vec{t}_i \times \vec{s}_i \right) \right) \left(\left(\left(\vec{P} + R\vec{b}_i - \vec{a}_i \right) \cdot R\vec{t}_i \right) \vec{s}_i \right) \right)^T$$

$$- \left(d_i^2 \left(\left(-\vec{s}_i \cdot R\vec{t}_i \right) \left(R\vec{t}_i \times \vec{s}_i \right) + \left(\left(R\vec{t}_i \times \vec{s}_i \right) \cdot R\vec{t}_i \right) \vec{s}_i \right) \right)^T$$

$$J_{A_1} = -\frac{1}{\sin\theta_i} \begin{bmatrix} 0\,0\,0 & \left(R\vec{t}_i \times \vec{s}_i \right)^T \end{bmatrix}. \tag{16}$$

Since a GSP mechanism can be designed by combining 6 constraints selected from 4 distance and 1 angular constraint types as given by Toz and Kucuk [9], the inverse Jacobian matrix of a GSP mechanism can also be constructed by using the related row vectors given in Eqs. (12)–(16).

4.2. Building inverse Jacobian matrices for 195 GSP mechanisms

In this section, the methodology for building the inverse Jacobian matrix of 195 GSP mechanisms is described by 2 examples: a symmetrical D_3^6 GSP mechanism composed of 6 legs, and a $D_1D_2D_3D_4A_1^2$ type asymmetrical GSP mechanism composed of 5 legs.

The D_3^6 GSP mechanism given in Figure 5 is a member of the 6D class given in [9]. It has 6 D_3 type constraints between the base and the moving platforms. The base platform of the mechanism is assembled by using 6 line segments that intersect at a common point O (the center of the base platform). The end points of the line segments are located on the circumferential circle of a hexagon whose corner points are labeled as $A_1A_2,\cdots,A_5$, and A_6. The moving platform of the mechanism is constructed by using the 6 points located on the circumferential circle of a hexagon and whose corner points were labeled as $B_1B_2,\cdots,B_5$, *and* B_6 The base and moving platforms were connected to each other by using the 6 C$\underline{\mathrm{P}}$S type legs whose active prismatic joints were labeled as $d_1d_2,\cdots,d_5$, *and* d_6. Since the mechanism is symmetrical, the 6 $\times$ 6 inverse Jacobian matrix of this mechanism is produced by using the row vector given in Eq. (14) six times as follows:

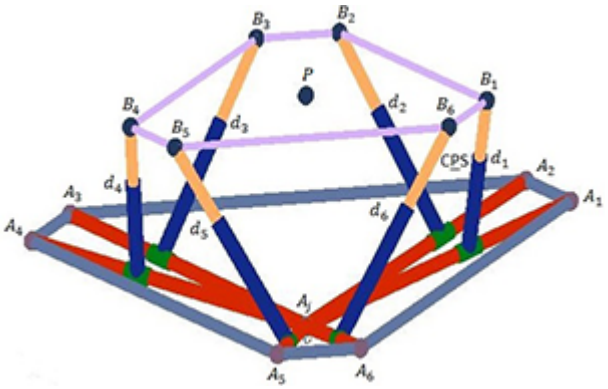

Figure 5. D_3^6 type symmetrical GSP mechanism.

$$J_{D_3^6} = \begin{bmatrix} J_{D_{3i}} & J_{D_{3i}} & J_{D_{3i}} & J_{D_{3i}} & J_{D_{3i}} & J_{D_{3i}} \end{bmatrix}^T \quad (i = 1, 2, \cdots, 6). \tag{17}$$

The $D_1D_2D_3D_4A_1^2$ GSP mechanism given in Figure 6 is a member of the 4D2A class and has 4 distance and 2 angular constraints between its base and moving platforms. In the figure, the constraints are provided by using 2 C$\underline{\mathrm{C}}$C, 1 S$\underline{\mathrm{P}}$S, 1 S$\underline{\mathrm{P}}$C, and 1 C$\underline{\mathrm{P}}$S type legs. Since the mechanism has 5 D_4 legs and 1 of the A_1 type, constraints are provided by 1 of the C$\underline{\mathrm{C}}$C type legs. The second cylindrical joint ($\underline{\mathrm{C}}$) of this leg performs both revolute and prismatic motion. The other C$\underline{\mathrm{C}}$C leg performs only revolute motion to produce the other A_1 type constraint, while the S$\underline{\mathrm{P}}$S, S$\underline{\mathrm{P}}$C, and C$\underline{\mathrm{P}}$S type legs perform prismatic motions to provide D_1, D_2, and D_3 type constraints, respectively. The related row vectors J_{D_1}, J_{D_2}, J_{D_3}, J_{D_4}, *and* J_{A_1} were obtained from Eqs. (12)–(16), and the 6 $\times$ 6 inverse Jacobian matrix of the $D_1D_2D_3D_4A_1^2$ type asymmetrical GSP mechanism was produced as follows:

$$J_{D_1D_2D_3D_4A_1^2} = \begin{bmatrix} J_{D_1} & J_{D_2} & J_{D_3} & J_{D_4} & J_{A_{11}} & J_{A_{12}} \end{bmatrix}^T. \tag{18}$$

It should be noted that although the mechanism has 5 legs, its inverse Jacobian matrix is a 6 $\times$ 6 matrix because of the defined 6 constraints between its base and moving platforms.

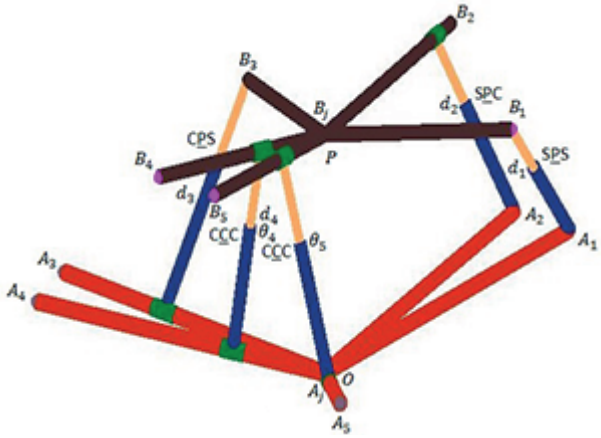

Figure 6. $D_1D_2D_3D_4A_1^2$ type 5 legs asymmetrical GSP mechanism.

4.3. Homogeneity of the inverse Jacobian matrices of 195 GSP mechanisms

The GSP mechanisms may have inhomogeneity between the elements of their Jacobian matrices. Since this inhomogeneity causes miscalculation of dexterity, the elements of the Jacobian matrices must be homogenized. Characteristic length [17] or weighting factor methods [19] are used to homogenize the elements of the Jacobian matrices. In order to homogenize the elements of the inverse Jacobian matrices, the units of the row vectors J_{D_1}, J_{D_2}, J_{D_3}, J_{D_4}, and J_{A_1} should first be determined, as in Eqs. (19)–(23):

$$UJ_{D_1} = [1\,1\,1\,m\,m\,m]_{1x6}, \tag{19}$$

$$UJ_{D_2} = [1\,1\,1\,m\,m\,m]_{1x6}, \tag{20}$$

$$UJ_{D_3} = [1\,1\,1\,m\,m\,m]_{1x6}, \tag{21}$$

$$UJ_{D_4} = [1\,1\,1\,m\,m\,m]_{1x6}, \tag{22}$$

$$UJ_{A_1} = [1\,1\,1\,1\,1\,1]_{1x6}, \tag{23}$$

where 1 means that the elements of the row vectors has no units, while m illustrates that the units of the elements of the row vectors are meters.

4.3.1. Numerical examples for D_3^6 and $D_1D_2D_3D_4A_1^2$ GSP mechanisms

Two numerical examples are also provided for D_3^6 and $D_1D_2D_3D_4A_1^2$ GSP mechanisms. The first example is presented for the D_3^6 GSP mechanism (Figure 5), whose coordinates of leg connection points located on the base and moving platforms are given in the Table. The goal position and orientation of the D_3^6 GSP mechanism are given as $P = \begin{bmatrix} p_x & p_y & p_z \end{bmatrix}^T = [10\,mm\ -10\,mm\ 138\,mm]^T$ and $(\alpha, \beta, \gamma) = (5^\circ, -5^\circ, -10^\circ)$, respectively. According to the Table, the inverse kinematics results of the active joint variables of the D_3^6 type GSP mechanism were obtained as follows: $d_1 = 143.909\,mm$, $d_2 = 132.988\,mm$, $d_3 = 155.211\,mm$, $d_4 = 123.512\,mm$, $d_5 = 126.31\,mm$, and $d_6 = 126.963\,mm$. Additionally, the inverse Jacobian matrix was computed by considering the characteristic length as 95 mm.

Table. Coordinates of leg connection points for D_3^6 type symmetrical and for $D_1D_2D_3D_4A_1^2$ type asymmetrical GSP mechanisms.

Mechanisms	Legs (i)	Coordinates of leg connection points on the platforms in mm											
		Base platform						Moving platform					
		$A_i\,(x,\,y,z)$			$A_j\,(x,\,y,z)$			$B_i\,(x,\,y,z)$			$B_j\,(x,\,y,z)$		
$D_1D_2D_3D_4A_1^2$ asymmetrical GSP	1	145.131	–20.932	30	*	*	*	64.147	–69.174	0	*	*	*
	2	145.131	20.932	30	*	*	*	145.131	69.174	0	0	0	0
	3	–54.437	136.153	30	0	0	0	27.833	90.14	0	*	*	*
	4	–90.693	115.221	30	0	0	0	–91.98	20.966	0	0	0	0
	5	–90.693	–115.221	30	0	0	0	–91.98	–20.966	0	0	0	0
D_3^6 symmetrical GSP	1	145.131	–20.932	30	0	0	0	64.147	–69.174	0	*	*	*
	2	145.131	20.932	30	0	0	0	64.147	69.174	0	*	*	*
	3	–54.437	136.153	30	0	0	0	27.833	90.14	0	*	*	*
	4	–90.693	115.221	30	0	0	0	–91.98	20.966	0	*	*	*
	5	–90.693	–115.221	30	0	0	0	–91.98	–20.966	0	*	*	*
	6	–54.437	–136.153	30	0	0	0	27.833	–90.14	0	*	*	*

$$J_{D_3^6} = \begin{bmatrix} 0.243 & 0.501 & -0.829 & 0.658 & 0.462 & 0.473 \\ 0.231 & -0.263 & -0.936 & -0.575 & 0.726 & -0.346 \\ -0.568 & -0.046 & -0.821 & -0.726 & 0.418 & 0.479 \\ 0.155 & 0.361 & -0.919 & -0.346 & -0.844 & -0.39 \\ 0.215 & -0.401 & -0.89 & 0.05 & -0.878 & 0.408 \\ -0.46 & -0.011 & -0.887 & 0.872 & 0.072 & -0.453 \end{bmatrix}. \tag{24}$$

The second example presented is for the $D_1D_2D_3D_4A_1^2$ GSP mechanism (Figure 6), whose coordinates of the leg connection points located on the base and moving platforms are illustrated in the Table. The goal position and orientation of the $D_1D_2D_3D_4A_1^2$ GSP mechanism are given as $P = \begin{bmatrix} p_x & p_y & p_z \end{bmatrix}^T = [7\,mm\ -8\,mm\ 124\,mm]^T$ and $(\alpha, \beta, \gamma) = (2^\circ, 5^\circ, -5^\circ)$, respectively. The inverse kinematics results of the active joint variables were obtained as follows: $d_1 = 133.007\,mm$, $d_2 = 87.5579\,mm$, $d_3 = 130.427\,mm$, $d_4 = 130.427\ mm$, $\theta_4 = 34.0845^\circ$, and $\theta_5 = 44.0236^\circ$. In addition, the inverse Jacobian matrix is computed by considering the characteristic length of 160 mm as follows:

$$J_{\mathrm{D_1D_2D_3D_4A_1^2}} = \begin{bmatrix} -0.599 & -0.457 & 0.656 & -0.084 & -0.645 & -0.527 \\ -0.106 & 0.181 & 0.977 & 0.283 & -0.781 & 0.176 \\ -0.533 & -0.026 & -0.845 & -0.458 & 0.161 & 0.284 \\ -0.08 & -0.309 & 0.947 & 0.102 & 0.311 & 0.11 \\ 0 & 0 & 0 & -0.08 & -0.309 & 0.947 \\ 0 & 0 & 0 & 0.058 & -0.294 & -0.953 \end{bmatrix}. \tag{25}$$

5. Conclusion

In this paper, the general equations for inverse Jacobian matrices of 195 6-DOF GSP mechanisms were symbolically obtained for 4 basic leg types considering 1 angular and 4 distance constraints. Since the 195 GSP mechanisms are designed by using combinations of these 4 basic leg types, verification of these general equations for all 195 GSP mechanisms can be made by only verifying the general equations of these 4 basic leg types. In addition, some types of GSP mechanisms ($D_4^3A_1^3$ is a member of 3D3A, and $D_1^5D_3$ is a member of 6D) given in this paper have also been studied by other authors. The inverse Jacobian matrices of these mechanisms were verified by comparison with the results given in these studies. Since the inverse Jacobian matrix of 195 GSP mechanisms may comprise several pages, the methodology for building the inverse Jacobian matrix was defined through 2 symmetrical and asymmetrical GSP mechanisms. The inhomogeneous elements of these matrices were also described. Finally, numerical examples for 2 different 6-DOF GSP mechanisms were also provided for illustrating the practical usefulness of the symbolically derived inverse Jacobian matrices. Since designing even one parallel manipulator is a very cumbersome issue, only a few types of 6-DOF GSP mechanisms have been designed and analyzed by researchers. With the help of the presented method and equations, researchers can easily design and analyze the 195 6-DOF GSP mechanism. These analyses may produce new and feasible 6-DOF GSP mechanisms for important specific tasks used in engineering, medical device design, and other applied branches.

References

[1] Merlet JP. Parallel Robots. Solid Mechanics and Its Applications Series. 2nd ed. Dordrecht, the Netherlands: Springer, 2006.

[2] Gao XS, Lei D, Liao Q, Zhang GF. Generalized Stewart–Gough platforms and their direct kinematics. IEEE T Robot 2005; 21: 141-151.

[3] Gan D, Liao Q, Dai JS, Wei S. Design and kinematics analysis of a new 3CCC parallel mechanism. Robotica 2010; 28: 1065-1072.

[4] Gan D, Liao Q, Wei S. Forward kinematics analysis of the new 3-CCC parallel mechanism. In: IEEE International Conference on Mechatronics and Automation; 5–8 August 2007; Harbin, Heilongjiang, China. Piscataway, NJ, USA: IEEE. pp. 905-910.

[5] Toz M, Kucuk S. Dimensional optimization of 6-DOF 3-CCC type asymmetric parallel manipulator. Adv Robotics 2014; 28: 625-637.

[6] Luo Y, Huang X, Zeng B. Forward displacement analysis of the 4SPS-2CCS generalized Stewart Platform based on hyper-chaotic neural network mathematical programming method. In: The 9th International Conference for Young Computer Scientists; 18–21 November 2008; Hunan, China. Piscataway, NJ, USA: IEEE. pp. 2857-2862.

[7] Luo Y, Xiao W, Zeng B, Huang X. Forward displacement analysis of the 5SPS-1CCS generalized Stewart Parallel robot mechanism based on hyper-chaotic methods. In: International Workshop on Chaos-Fractals Theories and Applications; 6–8 November 2009; Shenyang, China. Los Alamitos, CA, USA: IEEE. pp. 69-73.

[8] Luo YX, Che XY, Zeng B. Displacement analysis of the 3SPS-3CCS mechanism based on hyper-chaotic Newton-downhill method. Key Eng Mat 2011; 467–469: 401-406.

[9] Toz M, Kucuk S. Dexterous workspace optimization of an asymmetric six-degree of freedom Stewart–Gough platform type manipulator. Robot Auton Syst 2013; 61: 1516-1528.

[10] Gao Z, Zhang D, Ge Y. Design optimization of a spatial six degree-of-freedom parallel manipulator based on artificial intelligence approaches. Robot Cim-Int Manuf 2010; 26: 180-189.

[11] Ma O, Angeles J. Optimum architecture design of platform manipulators. In: Fifth International Conference on Advanced Robotics; 19–22 June 1991; Pisa, Italy. Piscataway, NJ, USA: IEEE. pp. 1130-1135.

[12] Kucuk S. A dexterity comparison for 3-DOF planar parallel manipulators with two kinematic chains using genetic algorithms. Mechatronics 2009; 19: 868-877.

[13] Lou Y, Liu G, Li Z. Randomized optimal design of parallel manipulators. IEEE T Autom Sci Eng 2008; 5: 1545-5955.

[14] Lara-Molina FA, Rosario JM, Dumur D. Multi-objective optimization of Stewart-Gough manipulator using global indices. In: IEEE/ASME International Conference on Advanced Intelligent Mechatronics; 3–7 July 2011; Budapest, Hungary. Piscataway, NJ, USA: IEEE. pp. 79-85.

[15] Bingul Z, Karahan O. Dynamic modeling and simulation of Stewart Platform. In: Kucuk S, editor. Serial and Parallel Robot Manipulators: Kinematics, Dynamics, Control and Optimization. Rijeka, Croatia: InTech, 2012. pp. 19-42.

[16] Liu H, Huang T, Chetwynd DG. A method to formulate a dimensionally homogeneous Jacobian of parallel manipulators. IEEE T Robot 2011; 27: 150-156.

[17] Angeles J. Fundamentals of Robotic Mechanical Systems Theory, Methods, and Algorithms. 3rd ed. New York, USA: Springer Science and Business Media, 2007.

[18] Fattah A, Ghasemi AMH. Isotropic design of spatial parallel manipulators. Int J Robot Res 2002; 21: 811-824.

[19] Hosseini MA, Daniali HRM, Taghirad HD. Dexterous workspace optimization of a tricept parallel manipulator. Adv Robotics 2011; 25: 1697-1712.

[20] Merlet JP. Jacobian, manipulability, condition number and accuracy of parallel robots. In: Thrun S, Brooks R, Durrant-Whyte H, editors. Robotics Research (Springer Tracts in Advanced Robotics). Heidelberg, Germany: Springer, 2007. pp. 175-184.